positioned, otherwise additional crosstalk is to be expected. For the tapered coupler, however, the crosstalk ratio can be maintained at an extremely low level as long as the device length is beyond certain length L ($L \approx 300$ μm in our example). Fig. 3 shows the spectral response of the said directional coupler filters. The solid line corresponds to the tapered coupler and the dash-dot line for the parallel one. It is seen that the linewidth of the tapered coupler in the example is slightly wider than the parallel one. However, the tapered coupler filter has much lower sidelobes compared with the parallel one. Here a reduction of the sidelobe level of about 10 dB is observed in the example examined. A further reduction of the sidelobes may be achieved by optimizing the shapes of the tapers as demonstrated in [9].

In conclusion, we have investigated the characteristics of the optical wavelength filters based on tapered directional couplers. In addition to its well-known effects in reducing the crosstalk and suppressing the sidelobes, the tapered structure can also be used to improve the length tolerance. An optimum design that can achieve low crosstalk, low sidelobes, and length-independent filter response may be realized.

References

[1] J. M. Senior and S. D. Cusworth, "Devices for wavelength multiplexing and demultiplexing," *IEE Proc.*, vol. 136, pt. J, pp. 183-202, 1989.

[2] S. S. Wagner and H. Kobrinski, "WDM applications in broadband telecommunication networks," *IEEE Comm. Mag.*, pp. 22-30, Mar. 1989.

[3] H. Kobrinski and K.-W. Cheung, "Wavelength-tunable optical filters: applications and technologies," *IEEE Comm. Mag.*, pp. 53-63, Oct. 1989.

[4] B. Broberg, B. S. Lindgren, M. G. Oberg, and H. Jiang, "A novel integrated optics wavelength filter in InGaAsP-InP," *J. Lightwave Technol.*, vol. LT-4, pp. 196-203, 1986.

[5] D. Marcuse, "Directional couplers made of nonidentical asymmetrical slabs. Part I: Synchronous couplers," *J. Lightwave Technol.*, vol. LT-5, pp. 113-118, 1987.

[6] H. C. Cheng and R. V. Ramaswamy, "A dual wavelength (1.32-1.56 μm) directional coupler demultiplexer by ion exchange in glass," *IEEE Photon. Technol. Lett.*, vol. 2, pp. 637-639, Sept. 1990.

[7] K. L. Chen and S. Wang, "Cross-talk problems in optical directional couplers," *Appl. Phys.*, vol. 44, pp. 166-168, 1984.

[8] H. A. Haus and N. A. Whitaker, Jr., "Elimination of cross talk in optical directional couplers," *Appl. Phys.*, vol. 44, pp. 1-3, 1985.

[9] R. C. Alferness and P. S. Cross, "Filter characteristics of codirectionally coupled waveguides with weighted coupling," *IEEE J. Quantum Electron.*, vol. QE-11, pp. 843-847, 1978.

[10] W. P. Huang and H. A. Haus, "Self-consistent vector coupled-mode theory for tapered optical waveguides," *J. Lightwave Technol.*, LT-8, pp. 922-926, 1990.

[11] W. P. Huang and B. E. Little, "Power exchange in tapered couplers," *IEEE J. Quantum Electron.*, to be published.

[12] B. E. Little, W. P. Huang, and S. K. Chaudhuri, "Effect of nonorthogonality on maximum power transfer in tapered couplers," *Opt. Lett.*, to be published.

An $N \times N$ Optical Multiplexer Using a Planar Arrangement of Two Star Couplers

C. Dragone

Abstract—**We describe the design of an integrated $N \times N$ multiplexer capable of simultaneously multiplexing and demultiplexing a large number (up to about 50) of input and output wavelength channels. The multiplexer is a generalization of the 2×2 Mach-Zehnder multiplexer. It consists of two $N \times M$ star couplers connected by M paths of unequal length. Aberrations caused by mutual coupling in the waveguide arrays are minimized by a correction scheme that causes each star coupler to accurately perform a Fourier transformation. The multiplexer should be useful as a wavelength routing device for long haul and local area networks.**

I. Introduction

We describe the design of an $N \times N$ multiplexer suitable for realization in integrated form for large N using the SiO_2/Si technology described in [1]-[3]. The multiplexer is a generalization of the 2×2 Mach-Zehnder multiplexer. It consists of two star couplers connected by M uncoupled waveguides having unequal lengths l_s forming a grating [5]-[8], as shown in Fig. 1. Each coupler is realized as in [1], [4] by using a planar arrangement of two confocal arrays of radial waveguides performing with efficiency approaching 100% under ideal conditions, when the waveguides have strong mutual coupling. Aberrations caused by mutual coupling ar minimized by a correction scheme which causes each star coupler to accurately perform a finite Fourier transformation. We show that it is possible, by using this scheme, to obtain good efficiency in the entire Brillouin zone of the grating, as demonstrated by the experimental results of a companion article [9]. Such a multiplexer should be useful as a wavelength routing device, for both long haul and local area networks. Its input-output mapping allows the same wavelength to be applied simultaneously to any number of

Manuscript received May 28, 1991.

The author is with AT&T Bell Laboratories, Crawford Hill Laboratory, Holmdel, NJ 07733.

IEEE Log Number 9102826.

1041-1135/91/0900-0812$01.00 © 1991 IEEE

Authorized licensed use limited to: Johns Hopkins University. Downloaded on November 13, 2008 at 17:19 from IEEE Xplore. Restrictions apply.

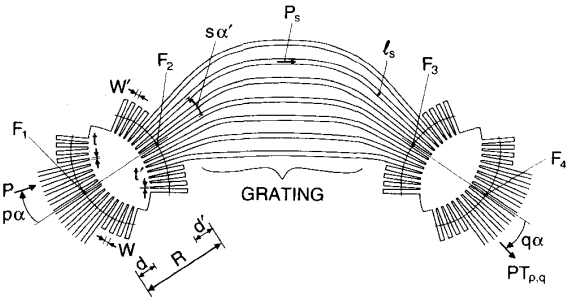

Fig. 1. An $N \times N$ multiplexer is realized using two identical couplers. The radial waveguides of each array emanate from one of the foci F_2.

input ports, with the corresponding signals appearing at different output ports. Thus, by employing N tunable lasers, each capable of N wavelengths, the multiplexer can be used as an $N \times N$ switch. Consideration will be restricted, in the following, to a grating of the type proposed in [6], but the correction scheme equally applies to other multiplexers [11], [12].

II. Multiplexer Design

The multiplexer of Fig. 1 is a symmetric arrangement of two identical couplers and a grating consisting of M uncoupled waveguides with propagation constant β. The first coupler consists of two periodic arrays of radial waveguides with foci F_1 and F_2. The waveguides are strips of constant refractive index n_2 separated by strips of index n_1. Each focus F_i is displaced (by d or d') from the circular boundary of the free-space region, which is characterized by uniform refractive index n_2. The input power P supplied to the pth port at a particular wavelength λ is transferred to the grating with efficiency $\epsilon_p = (\Sigma P_s)/P$ where P_s is the power in the sth arm. For an ideal multiplexer, entirely free of aberrations, the power transmission coefficient $T_{p,q}$ to the qth output port is $T_{p,q} = |\Sigma P_s \exp(j\phi_s)|^2/P^2$ where the phases ϕ_s are determined by the lengths l_s of the grating arms. By properly choosing these lengths, so as to effectively produce a constant path length difference l between adjacent paths, the difference $\phi = \phi_s - \phi_{s-1}$ becomes independent of s, and one finds that

$$\phi \simeq \beta l + kR(p - q)\alpha\alpha' \tag{1}$$

where α, α' are the angular separations between the waveguides of the two arrays (of either coupler) and R is the focal length F_1F_2. A simple relation is thus obtained between $T_{p,q}$ and the Fourier transform of P_s:

$$T_{p,q} = \epsilon_p\epsilon_q |h(\phi)|^2 \tag{2}$$

where

$$h(\phi) = [\Sigma P_s \exp(js\phi)]/(\Sigma P_s). \tag{3}$$

The above relation assumes that the multiplexer is entirely free of aberrations. Then, the multiplexer efficiency, given by the largest value of $T_{p,q}$, is just the product $\epsilon_q\epsilon_q$ of the efficiencies of the two couplers. This can be justified as follows. According to Lorentz reciprocity theorem, the transmission coefficient $T_{p,q}$ is determined by the coupling coefficient between two supermodes, produced in the grating (in opposite directions) by exciting the two ports p and q. By then assuming a perfect match (unity coupling) between the two modes, one obtains $T_{p,q} = \epsilon_p\epsilon_q$. This, however, requires two conditions. First, the various optical paths ϕ_s between the two ports p and q must be independent of s. Second, the relative powers P_s/P_o must differ by multiples of 2π. These conditions can be realized to a good approximation by optimizing the locations of the foci F_i as follows.

Consider, in the grating, the signals produced for $p = 0$ on a reference circle centered at F_1. According to [4], [5], mutual coupling between the input waveguides will affect the phases of these signals. It will cause phase errors $\delta\phi_s$, which must be minimized by optimizing F_1. The optimum F_1 can be determined as in [5], and it is called the phase center of the input array. Similarly, the optimum location of F_2 is the phase center of the second array. One can show, once the two foci are properly optimized, that each coupler becomes approximately equivalent to a confocal arrangement of two arrays without mutual coupling between the waveguides of each array [9] and, a consequence, one obtains approximately (1)–(3). Aberrations will not be entirely eliminated, however, by simply optimizing the two foci. It is therefore important, in general, to minimize residual aberrations by properly choosing the lengths l_s. The above conditions, optimizing respectively the two foci and the lengths l_s, complete our correction scheme. In general, a multiplexer with its foci displaced from their optimum locations, will have aberrations, reducing efficiency and increasing crosstalk, as shown in one of the examples given later. One can show that a small longitudinal displacement of F_1 will cause $\delta\phi_s \simeq k\delta d(\alpha' s)^2/2$. A displacement of F_2, on the other hand, will primarily affect the powers P_s. It will cause a lateral displacement $\delta x_p \simeq p\alpha\delta d'$ of the incident field illuminating the second array, thus causing P_s to vary with p.

We now point out a simple relation existing (approximately) between channel spacing ϕ_o, the total number N of channels in a period, and the focal length R. From (1)–(3), the transmission coefficient $T_{0,1}$ is displaced from $T_{0,0}$ by $\phi_o = kR\alpha\alpha'$. Furthermore, $h(\phi)$ is periodic with period 2π and, therefore, the total number of channels in a period is $\lambda/(R\alpha\alpha')$. This is also the total number of input waveguides in the central Brillouin zone of the grating. In fact, the angular width of this zone according to [5] is $\lambda/(R\alpha')$ and, therefore, dividing it by the angular spacing α, we obtain the desired result. Notice that N is not in general an integer, and it varies with λ.

Ideally, one would like the sidelobes of h to be very low and, at the same time, one would like N to be as large as possible, for a given M, so as to minimize the channel spacing, thus maximizing the total number of channels. The largest N is clearly M, and it can be realized efficiently by using efficient arrays, designed as in [4], [5] so that $P_s/P_o \simeq 1$. Then for $N \simeq M$

$$h \simeq \sin(N\phi/2)/[N \sin(\phi/2)]$$

giving the smallest channel spacing, which is then approxi-

Authorized licensed use limited to: Johns Hopkins University. Downloaded on November 13, 2008 at 17:19 from IEEE Xplore. Restrictions apply.

mately equal to the channel width determined by the 3 dB points of $|h|^2$. However, h in this case is afflicted by relatively high sidelobes. In order to substantially reduce them, one must increase the channel spacing by approximately a factor 1.7, and choose $M \simeq 2N$, as illustrated by the following examples.

III. Examples

Initially, let all arrays be designed efficiently as in [1], [2] by using SiO_2/Si waveguides with cores of width $W \simeq 5$ μm and $\Delta n \simeq 0.003$. In the vicinity of the free space regions, assume gaps t of 3 μm between the cores, and let the design wavelength be $\lambda_o \simeq \lambda/n = 1.3$ μm. The number N of input waveguides in the central Brillouin zone of the grating is determined by the focal length R. In the following example we choose $R \simeq 1350$ μm, resulting in $N \simeq 10$. By calculating the input array radiation characteristics, by a propagating beam method as in [5], one can determine the amplitudes and phases in the various arms of the grating. By then optimizing the location of F_1 one finds that the displacement of each phase center from the free-space region is accurately given by

$$\frac{d}{W} \tan \alpha \simeq 0.55$$

giving $d \simeq 350$ μm for $R = 1350$ μm. Fig. 2 shows the behavior of $T_{0,0}$ for a multiplexer optimized by the propagating beam method for $N = 10$ and $M = 11$. Also shown is the effect of reducing d by 200 μm. The resulting aberrations caused by mutual coupling substantially distort the main lobe, reducing efficiency and increasing crosstalk.

In the above example the input array approximately produced the same power in each arm of the grating. We next produce approximately a cosine distribution, so that $\sqrt{P_s/P_o} \simeq \cos(su)$, and optimize the parameter u by substantially increasing the width and the spacing $W + t$ of the input waveguides, thus reducing N. Reducing N from 10 to 7, and choosing $W \simeq 10$ μm and $t = 6$ μm, the sidelobes of h can be reduced to less than -25 dB as shown in Fig. 2. By also increasing M from 11 to 17, they can be further reduced to less than -36 dB, as illustrated in Figs. 2 and 3. The channel spacing now exceeds by a factor 1.7 the channel width, and this can be shown to be (approximately) the smallest channel spacing obtainable with sidelobes appreciably lower than -30 dB. The behavior of $T_{p,q}$ was found to agree with (1)–(3), for all values of p, q. Hence, the wavelength dependence was approximately independent of p, q and the efficiencies for $\phi = 0$ were accurately given by $T_{p,q} = \sqrt{T_{o,p}T_{o,q}}$ with

$$T_{o,q} = 0.944, 0.943, 0.927, 0.816, \text{ for } |q| = 0, \cdots, 3;$$

showing that the multiplexer performs well in the entire central zone of the grating, i.e., in the entire free spectral range determined by the period of $h(\phi)$. Notice that the marginal efficiencies for the input and output ports corresponding to the edges of the above zone are substantially lower, as expected because of Bragg reflections [4], [5].

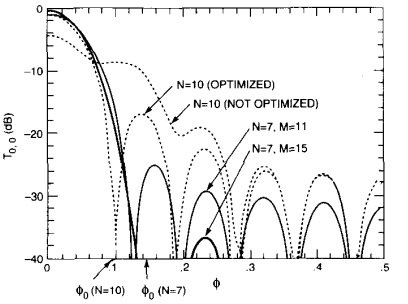

Fig. 2. The pattern of $T_{o,o}$ for a multiplexer optimized for $N = 10$ and $M = 11$ is compared with a nonoptimized pattern. Also shown are the optimized patterns $T_{o,o}$ for $N = 7$ and $M = 11$, 15.

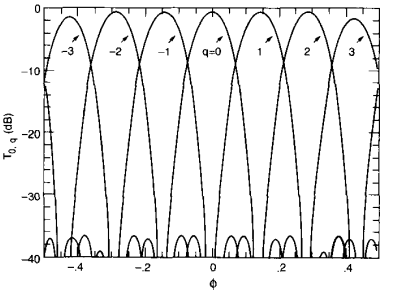

Fig. 3. Patterns $T_{o,p}$ for an optimized multiplexer with $N = 7$, $M = 15$.

IV. Conclusions

We have discussed the multiplexer performance for typical values of W and t. We have chosen a relatively small focal length $R \simeq 1350$ μm, resulting in $N = 7 - 10$. Greater N will be obtained by choosing a larger R, since N increases linearly with R, for given values of W and $W + t$. However, aberrations also increase linearly with R, and this must be taken into account in the design. Then, for large N, mutual coupling between the input and output waveguides is difficult to avoid, even for large N. Our technique then becomes particularly important. A companion paper [9] describes the measured performance of two multiplexers based on the above two designs.

Acknowledgment

I am indebted to J. M. Fernandes for her invaluable assistance.

References

[1] C. Dragone, C. H. Henry, I. P. Kaminow, and R. C. Kistler, "Efficient multichannel integrated optics star coupler on silicon," *IEEE Photon. Technol. Lett.*, vol. 1, pp. 241–243, 1989.

[2] C. H. Henry, G. E. Blonder, and R. F. Kazarinov, "Glass waveguides on silicon for hybrid optical packaging," *J. Lightwave Technol.*, vol. 7, pp. 1530–1939, 1989.

[3] N. Takato, K. Jinguji, M. Yasu, H. Toba, and M. Kawachi, "Silica-based single-mode waveguides on silicon and their application to guided-wave optical interferometers," *J. Lightwave Technol.*, vol. 6, pp. 1003–1010, June 1988.

[4] C. Dragone, "Efficiency of a periodic array with nearly ideal element pattern," *IEEE Photon. Technol. Lett.*, vol. 1, pp. 238–249, 1989.

[5] C. Dragone, "Optimum design of a planar array of tapered waveguides," *J. Opt. Soc. Amer. A.*, vol. 7, no. 11, pp. 2081–2093, Nov. 1990.

Authorized licensed use limited to: Johns Hopkins University. Downloaded on November 13, 2008 at 17:19 from IEEE Xplore. Restrictions apply.

[6] M. K. Smit, "New focusing and dispersive planar component based on an optical phased array," *Electron. Lett.*, vol. 24, pp. 385-386, 1988.
[7] A. R. Vellekoop and M. K. Smit, "Four-channel integrated-optic wavelength demultiplexer with weak polarization dependence," *J. Lightwave Technol.*, vol. 9, pp. 310-314, Mar. 1991.
[8] H. Takahashi, S. Suzuki, K. Kato, and I. Nishi, "Arrayed-waveguide grating for wavelength division multi/demultiplexer with nanometer resolution," *Electron. Lett.*, vol. 26, pp. 87-88, 1990.
[9] C. Dragone, C. A. Edwards, and R. C. Kistler, "Integrated optics $N \times N$ multiplexer on silicon," *IEEE Photon. Technol. Lett.*, to be published.
[10] C. Dragone, "Efficient $N \times N$ star coupler using fourier optics," *J. Lightwave Technol.*, vol. 7, pp. 479-489, 1989; see also C. Dragone, *Electron. Lett.*, vol. 24, pp. 942-943, 1988.
[11] J. B. D. Soole, A. Scherer, H. P. Leblanc, N. C. Andreadakis, R. Bhat, and M. A. Koza, "Monolithic InP-based grating spectrometer for wavelength-division multiplexed systems at 1.5 μm," *Electron. Lett.*, vol. 27, no. 2, pp. 132-134, Jan. 1991.
[12] J. Lipson, W. J. Minford, E. J. Murphy, T. C. Rice, R. A. Linke, and G. T. Harvey, "A six-channel wavelength multiplexer and demultiplexer for single mode systems," *J. Lightwave Technol.*, vol. LT-3, pp. 1159-1163, 1975.

An InGaAs/InAlAs Superlattice Avalanche Photodiode with a Gain Bandwidth Product of 90 GHz

Toshiaki Kagawa, Hiromitsu Asai, and Yuichi Kawamura

Abstract—**This letter describes the fabrication of an InGaAs/InAlAs superlattice avalanche photodiode with a gain bandwidth product of 90 GHz. The device is composed of an InGaAs/InAlAs superlattice multiplication region and an InGaAs photoabsorption layer. The effect of the superlattice multiplication region thickness on the gain bandwidth product is studied. A gain bandwidth product of 90 GHz is obtained for the device with a multiplication region thickness of 0.52 μm.**

IMPACT ionization rates, which strongly affect performances of avalanche photodiodes (APD's), can be controlled by introducing a superlattice (SL) structure into the multiplication region [1]. The electron ionization rate significantly increases in InGaAs/InAlAs SL [2]. The increased ratio of electron ionization rate to holes increases the gain bandwidth (GB) product while reducing multiplication noise. A separate absorption and multiplication (SAM) SL-APD using InGaAs/InAlAs SL as a carrier multiplication region with an extremely low multiplication noise was fabricated [3]. An optical receiver using this APD has the highest sensitivity to 10 Gb/s signal ever reported for receivers using APD's [4], [5].

The GB product of APD is the most important factor which determines the sensitivity of a receiver for an optical transmission system operating at a high bit rate. The GB product is a function of the ionization rate ratio and the carrier transit time in the multiplication region. The transit time in the multiplication region is determined by the thickness of the region and the carrier velocity. The relationship between the GB product and the multiplication region thickness, however, has not been reported for SL APD. This letter reports the effect of the multiplication region thickness on the GB product for the first time. Two kind of devices with a multiplication region thicknesses of 0.68 and 0.52 μm are fabricated and the GB products of these devices are compared. The device with the 0.52 μm thick multiplication region has a GB product of 90 GHz.

The epitaxial wafers were prepared by the molecular beam epitaxy. The layer structure is shown in Fig. 1. The nondoped InGaAs/InAlAs SL was grown on Si-doped n^+-SL and InAlAs buffer layers. Three p-InGaAs layers with different Be-doping concentrations were grown. The first layer, the sheet-doped layer, had a thickness of 16 nm and a doping concentration of 8×10^{17} cm^{-3}. The second layer, the photoabsorption layer, had a thickness of 1.7 μm. This layer was quite lightly Be-doped to a concentration of 2×10^{15} cm^{-3}. The sheet-doped layer is used to control the difference between the electric field strength of the SL multiplication region and that of the photoabsorption layer [3]. The third layer was highly doped (1×10^{18} cm^{-3}) and has a thickness of 0.1 μm. Then Be-doped p^+-InAlAs window and p^+-InGaAs ohmic contact layers were grown.

The well and barrier layers of SL were both 20 nm thick. Two kind of devices with different SL periods were prepared. Devices *A* and *B* had SL periods of 13 and 17, respectively. The total thicknesses of the SL multiplication region were, consequently, 0.52 and 0.68 μm, respectively.

Manuscript received April 24, 1991; revised June 28, 1991.
The authors are with NTT Opto-electronics Laboratories, Kanagawa 243-01, Japan.
IEEE Log Number 9102742.

1041-1135/91/0900-0815$01.00 © 1991 IEEE

Authorized licensed use limited to: Johns Hopkins University. Downloaded on November 13, 2008 at 17:19 from IEEE Xplore. Restrictions apply.